Experimental and Theoretical Study of the Spin−Spin Coupling Tensors in Methylsilane

Jaakko Kaski,[†] Perttu Lantto, Tapio T. Rantala, Jyrki Schroderus, Juha Vaara,[‡] and Jukka Jokisaari*

Department of Physical Sciences, University of Oulu, P.O. Box 3000, FIN-90401 Oulu, Finland

Received: June 21, 1999; In Final Form: September 13, 1999

The experimental and theoretical $^{13}C-^{29}Si$ spin−spin coupling tensors, $^1\mathbf{J}_{CSi}$, are reported for methylsilane, $^{13}CH_3{}^{29}SiH_3$. The experiments are performed by applying the liquid crystal NMR (LC NMR) method. The data obtained by dissolving CH_3SiH_3 in nematic phases of two LC's is analyzed by taking into account harmonic and anharmonic vibrations, internal rotation, and solvent-induced anisotropic deformation of the molecule. The necessary parameters describing the relaxation of the molecular geometry during the internal rotation, as well as the harmonic force field, are produced theoretically with semiempirical (AM1 and PM3) and ab initio (MP2) calculations. A quantum mechanical approach has been taken to treat the effects arising from internal rotation. All the **J** tensors are determined theoretically by ab initio MCSCF linear response calculations. The theoretical and experimental **J** coupling anisotropies, $\Delta^1J_{CSi} = -59.3$ Hz and -89 ± 10 Hz, respectively, are in fair mutual agreement. These results indicate that the indirect contribution has to be taken into account when experimental $^1D_{CSi}{}^{exp}$ couplings are to be applied to the determination of molecular geometry and orientation. The theoretically determined **J** tensors are found to be qualitatively similar to what was found in our previous calculations for ethane, which suggests that the indirect contributions can be partially corrected for by transferring the corresponding **J** tensors from a model molecule to another.

Introduction

The spin−spin coupling tensor, $\mathbf{J}_{ij}$, between the nuclei *i* and *j* of a molecule is a second-order tensor property formed by the response of the electron system to perturbing nuclear magnetic moments. The isotropic spin−spin coupling constant, J_{ij}, is the average of the diagonal terms of $\mathbf{J}_{ij}$, i.e., one-third of the trace of the tensor. It is usually easy to determine experimentally using nuclear magnetic resonance (NMR) spectroscopy, as it appears in the ordinary isotropic liquid (or gas) phase.

Establishing the anisotropy of the **J** tensor, $\Delta J = J_{zz} - {}^1/_2(J_{xx} + J_{yy})$, with respect to a suitably chosen *z*-axis, is a demanding task that is experimentally possible by applying either the liquid crystal (LC) NMR[1,2] or solid-state NMR method.[3] The former is the most applicable in the case of relatively small spin−spin coupling anisotropies, as the information is easily masked by broad lines in the latter. In either NMR method, the experimentally observable anisotropic coupling, D^{exp}, contains contributions from the direct dipolar coupling, *D*, which contains information on the internuclear distances and the orientation of the internuclear vector with respect to the magnetic field, and the indirect spin−spin coupling. Thus, the experimental determination of molecular geometry parameters and orientation from the experimental NMR data requires that the number of free parameters is equal to or smaller than the number of couplings for which the indirect contribution is small or known. This information can be used to calculate the direct part of the remaining couplings. The difference between the experimental and calculated coupling gives the orientation-dependent indirect contribution, J^{aniso}. In the case of experimental HH and CH couplings, the indirect contributions to the corresponding experimental $D_{ij}{}^{exp}$ couplings are less than 1%.[1] There may be exceptions to this, if the direct part of the experimental coupling vanishes.[4] However, a large relative contribution, ${}^1/_2J_{ij}{}^{aniso}/D_{ij}{}^{exp}$, due to vanishing or small denominator does not lead to serious errors, if the analysis of the molecular properties is overdetermined.[5] Based on experience gained in studies of several model systems, if the maximum acceptable errors are 0.5% in the internuclear distances and 0.5° in bond angles, the indirect contributions can safely be ignored in the experimental HH, CH, CC, and HF couplings.[1,5−7] The situation is similar for $^1\mathbf{J}_{CF}$ and $^2\mathbf{J}_{FF}$,[4,5] whereas in the cases of $^2\mathbf{J}_{CF}$, $^3\mathbf{J}_{CF}$, $^4\mathbf{J}_{CF}$, and $^5\mathbf{J}_{FF}$, the indirect contribution to the corresponding D^{exp} coupling may be significant. This depends on the molecular orientation, because the direct and indirect coupling tensors do not possess the same principal axis system in general.

Recently, the utility of residual dipolar couplings in the derivation of structural information on weakly aligned biomacromolecules has been recognized and the field is gaining growing interest.[8] The reliable use of the NMR data, however, necessitates consideration of various contributions, such as molecular vibrations,[9] correlation of vibrational and reorientational motions (the so-called orientation-dependent deformation effects),[10] and spin−spin coupling tensor, in the experimental dipolar couplings, D^{exp}, as seen below. Applications of the LC NMR method to large molecules are often limited by the availability of at least the harmonic force field (FF), which is necessary for performing both the vibrational and deformational corrections. This paper deals with the spin−spin coupling tensors in methylsilane, but we also investigate the significance of the quality of the harmonic FF by applying the results of both semiempirical and ab initio electronic structure methods. They

* Author for correspondence. Fax: +358-8-553 1287. Tel: +358-8-553 1308. E-mail: Jukka.Jokisaari@oulu.fi.

[†] Present address: Oulu Polytechnic, Raahe Institute of Computer Engineering, P.O. Box 82, FIN-92101 Raahe, Finland.

[‡] Present address: Max-Planck-Institut für Festkörperforschung, Heisenbergstrasse 1, D-70569 Stuttgart, Germany.

10.1021/jp9920491 CCC: $18.00 © 1999 American Chemical Society
Published on Web 11/12/1999

are compared with the results obtained by using a scaled Hartree−Fock level FF taken from ref 11. This test gives useful information on the applicability of the semiempirical methods, which are fast and, thus, usable also for quite large molecules.

The spin−spin coupling anisotropies of methylsilane are fundamentally interesting as they serve as an opportunity to expand the general view on **J** tensors by examining their change when carbon is substituted with silicon, which belongs to the same column in the periodic table of elements. Molecules containing similar structural units have related isotropic spin−spin coupling constants, but an important question is whether the anisotropic properties of **J** have similarities as well. In the present study, we obtain some information for answering to this. However, reliable sets of **J** tensors are available for quite few molecules. The experimental and theoretical results are in good mutual agreement for some model systems (HCN, HNC, CH_3-CN, and CH_3NC,[12] C_6H_6,[6] C_2H_6, C_2H_4, and C_2H_2,[7] CH_3F, CH_2F_2, and CHF_3,[5] and 1,4-$C_6H_4F_2$[4]) containing light atoms. This implies that the theoretical **J** tensors are reliable at least for small molecules consisting of fluorine and other first-row main group atoms. Thus, the theoretical **J** tensors of, e.g. formamide,[13] for which experimental data are not available, are most likely reliable. These theoretical calculations encompass also couplings to oxygen. In systems containing heavier nuclei, from the third row of the periodic table on, relativistic effects on spin−spin coupling tensors become more important.[14−16] Although the performance of ab initio methods is not yet at a satisfactory level, the DFT method has proved to be capable of producing **J** tensors with reasonable degree of accuracy for this kind of systems.[17]

In the theoretical calculations, the spin−spin coupling tensor is obtained from the terms of the perturbation Hamiltonian that are bilinear in the nuclear spins $\mathbf{I}_i$ and $\mathbf{I}_j$, or (in the second order) linear in one of these. Consequently, there are five different contributions at the nonrelativistic level that, in the language of the response theory,[18] can be expressed as linear response functions. Exception to this is the diamagnetic spin−orbit tensor (DSO) that is a ground-state expectation value and hence easy to calculate. The paramagnetic spin−orbit mechanism (PSO) couples the ground state with singlet excited states, necessitating solution of three linear response equations for each nucleus. The main computational challenge is the many triplet linear response calculations needed for accounting for the spin-dipolar (SD), the fully isotropic Fermi contact (FC), and the fully anisotropic spin-dipolar/Fermi contact cross (SD/FC) mechanisms. Particularly, the SD contribution is laborious to calculate, as one is obliged to solve nine (six if the symmetry is considered) linear response equations for each nucleus. The triplet response functions require the use of a reference state that is stable against triplet excitations. These can be obtained using correlated MCSCF or coupled cluster (CC) methods. When using the MCSCF linear response method, large restricted active space (RAS) wave functions are usually required in order to take electron correlation effects sufficiently into account. In addition to this, the spin−spin coupling necessitates sufficient flexibility from the basis set in core regions as the recently reported systematic investigation also ascertained.[19] The high requirements for the quality of the description of the electronic structure make these calculations especially demanding among molecular properties. As a result, reliable **J** tensors and sufficiently precise self-supporting data have been obtainable only during recent years. Currently, the quality of the theoretical results makes them good starting values for the analysis of the experimental data. Similarly, calculations can provide trustworthy comparison data in the case of the anisotropic properties of the **J** tensor.

In the present study we investigate the methylsilane molecule using LC NMR experiments and ab initio MCSCF linear response calculations. Experimentally, we have fitted the molecular geometry and Δ^1J_{CSi} to the LC NMR data. The contributions arising from the molecular rovibrational motion to the D^{exp} couplings are taken into account in the analysis. The harmonic force field, used in the derivation of the motional contributions, is produced using different methods in order to obtain insight to the applicability of the semiempirical methods for this purpose. Experimental information on **J** tensors is compared with the ab initio MCSCF results, and the transferability of the tensors to other molecules is discussed.

The analysis of the experimental data of methylsilane is relatively complicated due to the internal rotation of the molecule, which averages the $^3D_{HH}^{cis}$ and $^3D_{HH}^{trans}$ couplings between the methyl and silyl groups. In our previous investigation of the related ethane molecule,[7] all relevant effects due to the internal rotation were taken into account. In that case, the analysis of the LC NMR data was relatively laborious as it involved a description of the various contributions to the direct couplings in terms of Fourier expansion as a function of the rotation angle, necessitating a systematic scan of the coupling parameters. In the present case, we have developed the data analysis method to be more automatic.

Theory

NMR Observables. The NMR spin Hamiltonian in frequency units as appropriate for spin-$^1/_2$ nuclei in molecules partially oriented in uniaxial LC solvents can be written, in the high field approximation, as

$$\hat{H} = -B_0/(2\pi)\sum_i \gamma_i(1-\sigma_i)\hat{I}_{iz'} + \sum_{i<j} J_{ij}\hat{\mathbf{I}}_i\cdot\hat{\mathbf{I}}_j + \sum_{i<j}(D_{ij} + {}^1/_2 J_{ij}^{aniso})(3\hat{I}_{iz'}\hat{I}_{jz'} - \hat{\mathbf{I}}_i\cdot\hat{\mathbf{I}}_j) \quad (1)$$

where B_0 is the magnetic field of the spectrometer (in the z' direction), γ_i, $\hat{\mathbf{I}}_i$, and σ_i are the gyromagnetic ratio, dimensionless spin operator, and nuclear shielding (sum of the isotropic and anisotropic contributions), of nucleus i, respectively. The direct dipolar coupling D_{ij} is defined as

$$D_{ij} = -\frac{\mu_0\hbar\gamma_i\gamma_j}{8\pi^2}\left\langle\frac{s_{ij}}{r_{ij}^3}\right\rangle \quad (2)$$

where the time averaging is indicated by the angular brackets and μ_0 and $\hbar$ have their usual meanings. The orientational order parameter, S_{ij}, of the internuclear $\mathbf{r}_{ij}$ vector is closely related to the eq 2 by $S_{ij} = \langle s_{ij}\rangle = {}^1/_2\langle 3\cos^2\theta_{ij,\mathbf{B}_0} - 1\rangle$, where $\theta_{ij,\mathbf{B}_0}$ is the angle between the $\mathbf{r}_{ij}$ vector and the direction of the external magnetic field $\mathbf{B}_0$. One should note that $\langle s_{ij}/r_{ij}^3\rangle$ is not equal to $S_{ij}/\langle r_{ij}^3\rangle$ due to the orientation-dependent deformation of the solute (similarly, $\langle r_{ij}^{-3}\rangle^{-1/3} \neq r_{ij}$). Thus, the experimental couplings of a molecule in a LC solvent can be expressed as a sum of several contributions:

$$D_{ij}^{exp} = D_{ij} + {}^1/_2 J_{ij}^{aniso} = D_{ij}^{eq} + D_{ij}^{ah} + D_{ij}^{h} + D_{ij}^{d} + {}^1/_2 J_{ij}^{aniso} \quad (3)$$

where D_{ij}^{eq} is the coupling corresponding to the equilibrium structure of the molecule, D_{ij}^{ah} arises from the anharmonicity of the vibrational potential,[20] D_{ij}^{h} is the contribution from the

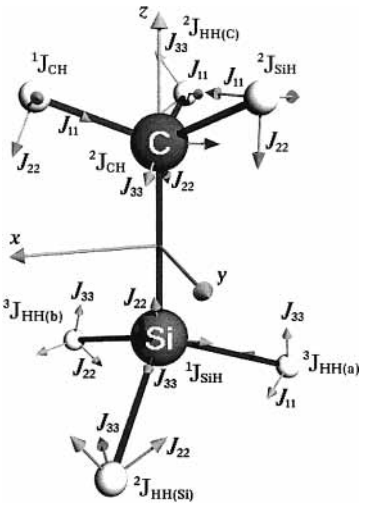

Figure 1. Methylsilane and the principal axis systems of its spin−spin coupling tensors. The *x* axis is in the HCSiH plane, where the protons are the ones for which the PAS of the $^1J_{CH}$ and $^3J_{HH(a)}$ tensors are shown (in the respective order).

harmonic vibrations,[9] and D_{ij}^{d} is the deformational contribution.[10] The anisotropic contribution due to the **J** tensor is given by

$$J^{\text{aniso}} = (2/3)P_2(\cos\theta)\sum_{\alpha\beta} S^D_{\alpha\beta} J_{\alpha\beta} \tag{4}$$

where $S^D_{\alpha\beta}$ are the elements of the Saupe orientation tensor with respect to the LC director **n**, expressed in a molecule-fixed frame (*x*, *y*, *z*). P_2 is the second-order Legendre polynomial, $\delta_{\alpha\beta}$ is the Kronecker delta, and θ the angle between $\mathbf{B}_0$ and **n**. In the present case of C_{3v} molecular point group symmetry, eq 4 is expressed as

$$J^{\text{aniso}} = (2/3)P_2(\cos\theta)S^D_{zz}\,\Delta J \tag{5}$$

The orientation tensor is calculated from the traceless solvent−solute interaction tensors, **A**,[10c] assigned to the chemical bonds of a molecule. In the present case, the fitted interaction tensors are $\mathbf{A}_{CH}$, $\mathbf{A}_{SiH}$, and $\mathbf{A}_{CSi}$, which were assumed to be cylindrically symmetric in the corresponding bond directions. The use of interaction tensors has been documented in detail in ref 10c.

Internal Rotation. We used the program MASTER[21] to calculate the molecular orientation and D^{eq}, D^{h}, and D^{d} couplings (see eq 3) from the molecular geometry, harmonic force field, and the interaction tensors. Anharmonic vibrations are taken into account by using the AVIBR program[20] for other than the torsional degree of freedom that causes the averaging of the $^3D_{HH}^{exp}$. The effect arising from the torsional motion is calculated numerically with the equation

$$\langle D\rangle = \int_0^{\pi/3} D(\phi)p(\phi)\,\mathrm{d}\phi \tag{6}$$

where $D(\phi)$ is the direct coupling (including all contributions) as a function of the internal rotation angle and $p(\phi)$ is the corresponding normalized probability distribution function at a given temperature. The changes of the geometrical parameters as function of the internal rotation are taken into account on the basis of semiempirical and ab initio electronic structure calculations that are used to produce also the harmonic force field as a function of ϕ. In Figure 1, the molecule and the molecule-fixed coordinate frame used are shown. In the figure, the molecule is in the equilibrium geometry, where $\phi = 0$.

The function $p(\phi)$ that describes the probability of finding the torsional oscillator at a given torsional angle was calculated by using the torsional wave functions obtained using the vibrational−torsional Hamiltonian

$$\hat{H}_{\text{vtr}} = \sum_i \omega_i\left(v_i + \frac{d_i}{2}\right) + F\hat{p}^2 + \frac{1}{2}V_3(1-\cos 3\phi) \tag{7}$$

where ω_i is the vibrational frequency, v_i is the vibrational quantum number, and d_i is the degeneracy of the vibrational mode *i*. The last two terms belong to the pure torsional Hamiltonian, where *F* is the reduced rotational constant and V_3 is the first term in the Fourier expansion of the torsional barrier height. Operator $\hat{p}$ is the torsional angular momentum and $1/2V_3(1-\cos 3\phi)$ is the torsional potential term. The last two terms in operator (7) were used to set up the torsional matrix in the free rotor basis. As a result, the following eigenfunctions are obtained:

$$\Psi(v_6,\tau,\phi) = \sum_{k=-10}^{10} A^{v_6}_{3k+\tau}\exp[\mathrm{i}\phi(3k+\tau)] \tag{8}$$

In eq 8, v_6 is the torsional principal quantum number, τ is a label for the torsional sublevels, and *k* is the free rotor quantum number. The probability density of the torsional oscillator can be calculated as $|\Psi|^2$.

In order to obtain a probability distribution to describe the statistical ensemble of torsional oscillators, the energy manifold given by the eigenvalues of the operator (7) was used. The energy level structure consists of various combinations of all the fundamental vibrations including the stack of torsional levels and sublevels. The energies beyond 3000 cm^{-1} do not give any statistically significant contribution to the population, and they were neglected from the total probability density. The torsional parameters *F* and V_3 were assumed to be independent of the vibrational states.

The normalized probability distribution function is

$$p(\phi) = \frac{\sum_{v,v_6,\tau} d_v \exp\{-E(v,v_6,\tau)/k_BT\}|\Psi(v_6,\tau,\phi)|^2}{\sum_{v,v_6,\tau} d_v \exp\{-E(v,v_6,\tau)/k_BT\}} \tag{9}$$

where k_B is the Boltzmann constant and *T* is the temperature. *E* is the eigenvalue of operator (7) and *v* represents the combination (v_1, v_2, ..., v_5, v_7, ..., v_{12}) of the vibrational quantum numbers, i.e., the total vibrational quantum number. The quantity d_v is the degeneracy of the corresponding state, and the denominator is the partition function at temperature *T*. The experimental values for the vibrational frequencies were taken from ref 22 and the torsional parameters $F = 8.207\,14$ cm^{-1} and $V_3 = 603$ cm^{-1} for $^{12}CH_3{}^{28}SiH_3$ were taken from ref 23.

Experiments and Computational Details

Experiment. Methylsilane (^{13}C and ^{29}Si in natural abundance) was prepared by reacting methylsilyl trichloride with $LiAlH_4$.[24] The LC solvents Merck ZLI 1167 and ZLI 2806 were placed into NMR sample tubes (Wilmad) of 10 mm outer diameter and 1.5 mm wall thickness, and degassed before methylsilane was condensed into them. Then the tubes were sealed with flame. The gas pressures were approximately 12 atm at room temperature. The NMR spectra were recorded on a Bruker Avance DSX 300 spectrometer. For the determination of the

isotropic spin−spin coupling constants for each sample, ^{1}H, ^{13}C, ^{29}Si, and ^{13}C−{^{1}H} spectra were measured at temperatures slightly above the nematic−isotropic phase transition. The sufficient signal-to-noise ratio was reached after 64, 2000, 800, and 4000 scans, respectively. The isotropic ^{13}C−^{29}Si spin−spin coupling constant was extracted from the ^{13}C−{^{1}H} spectrum by applying total-line-shape (T) mode in the iterative PERCH program.[25] The other J_{ij} couplings were analyzed by incorporating the ^{1}H, ^{13}C, and ^{29}Si spectra of a sample to the same analysis and by using the T mode. The values were fixed to those obtained at temperatures where the samples are in the isotropic phase. For determination of the complete set of D_{ij} couplings, only the ^{13}C−{^{1}H} spectrum with ^{29}Si satellites and the ^{1}H spectrum with ^{13}C and ^{29}Si satellites were needed. The proton irradiation of the ^{13}C−{^{1}H} experiment tends to heat the sample, which forced us to use short accumulation (irradiation) time of 0.38 s and long relaxation delay of 2.0 s with gated decoupling. The power used in the proton irradiation was set to as low as possible. The temperature-dependent orientation of the solute molecules during the ^{13}C−{^{1}H} accumulation was checked and found unchanged by measuring the ^{1}H spectrum with one scan (enough for the $^{12}CH_3{}^{28}SiH_3$ isotopomer) immediately after the end of the irradiation experiment. The ^{13}C−{^{1}H} spectrum was analyzed with the T mode, whereas the ^{1}H spectrum, consisting of spectra of three isotopomers, was analyzed with peak-top-fit mode, assuming the same orientations for $^{13}CH_3{}^{28}SiH_3$ and $^{12}CH_3{}^{29}SiH_3$ isotopomers.

Molecular Vibrational Potential. To assess the effects arising from molecular vibration to the observed NMR parameters, the harmonic force field of the molecule was calculated using the Gaussian software[26] at the semiempirical level with two parametrizations AM1[27] and PM3,[28] and at the ab initio (MP2)[29] level. The force fields from different methods serve in finding trends (and hopefully convergence) as the level of sophistication of the method of calculation is improved.

Three different conformations were considered. The calculations of the harmonic force fields and relaxed molecular geometries were performed at the internal rotation angles of 0°, 30°, and 60°. Due to the C_{3v} symmetry, this range determines the full 360° rotation. The force constants representing the torsional vibration were ignored in MASTER, but they were taken into account when applying eq 6.

In the semiempirical calculations, only the outermost s and p electrons of each atom are treated explicitly, amounting to total of 14 valence electrons in the molecular orbitals of CH_3-SiH_3. At the MP2 level, all-electron calculations were carried out and the basis set was enlarged until sufficient convergence was found at the 6-311+G(d,p) level.

Ab initio Calculations of J Tensors. The spin−spin coupling tensors were calculated with the MCSCF linear response method[30] implemented in the Dalton software.[31] For details, we refer to the original paper and a recent review.[32]

Two restricted active space (RAS) MCSCF wave functions were chosen on the basis of natural orbital occupation numbers obtained from MP2 analysis. Using the nomenclature ${}^{\text{inactive}}\text{RAS}^{\text{RAS2}}_{\text{RAS3}}$ adopted from ref 33, the smaller RAS-I wave function is ${}^{51}\text{RAS}^{52}_{10;5}$ and the larger RAS-II wave function is ${}^{51}\text{RAS}^{52}_{21;13}$. The numbers in each category express the orbitals belonging to A′ and A″ irreps of the Abelian C_s point group and in the SCF wave function these symmetries contain 10 and 3 occupied orbitals. Both RAS wave functions were of the single-reference type, as static correlation is expected to be relatively unimportant in this kind of singly bonded system (at the equilibrium geometry). Single and double excitations were allowed from the occupied (in the SCF picture) valence molecular orbitals (MOs) belonging to the RAS2 subspace to the virtual MOs in RAS3. We kept six core MOs consisting of the 1s AO of the carbon atom and 1s, 2s, and 2p AOs of the silicon atom inactive. The active spaces in the RAS-I and RAS-II wave functions consist of orbitals containing 71.7% and 94.4% of all virtual MP2 particles and the number of the Slater determinants was 7956 and 40 669, respectively. All the nonrelativistic terms were determined at each level of calculation.

TABLE 1: Basis Sets Used in the Ab Initio Calculations[a]

basis	element	Gaussians
HII	H	[5s1p/3s1p]
	C	[9s5p1d/5s4p1d]
	Si	[11s7p2d/7s6p2d]
HIII	H	[6s2p/4s2p]
	C	[10s7p2d/7s6p2d]
	Si	[12s8p3d/8s7p3d]

[a] Spherical Gaussians are used throughout. Only the innermost primitives of a given type are contracted.

Basis set convergence was studied with the larger active space by using two basis sets, HII and HIII, originally adopted from Huzinaga[34] and modified by Kutzelnigg and co-workers.[35] As noticed earlier, the latter set provides well-converged spin−spin couplings with a fairly small number of basis functions.[19,36] The basis sets are listed in Table 1. The experimental r_0 geometry[37] was used in the calculations.

Results

Experimental Spin−Spin Coupling Tensors. Some of the isotropic spin−spin coupling constants and their signs of methylsilane are reported in the literature. For example, $^1J_{\text{SiH}}$ is negative[38] and values of (−)194.3 and (−)193.0 Hz are reported in ref 39. $^1J_{\text{CSi}}$ is most likely negative because the similar coupling in the TMS molecule is about −50 Hz.[39] $^2J_{\text{SiH}}$ is known to be positive and in the range from 3 to 10 Hz.[38] This information, combined with the fact that $^1J_{\text{CH}}$ is positive, enables us to determine each observable J coupling of methylsilane with their signs from the NMR spectra taken from isotropic and anisotropic phases. The experimental J_{ij} couplings in LC's ZLI 1167 and ZLI 2806 are given in Table 2 and the sets of the experimental D_{ij} couplings are given in Table 3.

In the analysis of the data by applying eq 6, the relaxation of a geometrical parameter was scaled with the same ratio as the theoretical parameter by using

$$P(\phi) = (P_{\text{iter}}/P_{\text{theor}})[a_0 + a_1\cos(n\phi) + a_2\cos(2n\phi)] \quad (10)$$

Here $n = 3$ due to the symmetry and $P(\phi)$ is a geometrical parameter (bond length or angle) as function of the internal rotation ϕ. (One should point out that $D(\phi)$ in eq 6 is a function of P's.) P_{iter} is obtained from the fit to D^{exp} couplings, while P_{theor}, corresponding to the torsional angle $\phi = 0$, is given by semiempirical or ab initio calculations. The coefficients a_0, a_1, and a_2 are fitted a priori to describe the theoretical molecular geometry at 0°, 30°, and 60° of internal rotation angle and these values are used to calculate the theoretical geometrical parameters at any ϕ. The a's are given in Table 4.

The harmonic force field was given by the theoretical calculations in Cartesian coordinates, but the force constants change significantly as functions of the torsional angle and the systematics of the functions is complicated. Therefore, the interpolation of the FF to a given ϕ would have been difficult. The easiest way to avoid this problem was to use the FF in the

TABLE 2: Experimental and Theoretical Isotropic J_{ij} Coupling Constants of Methyl Silane in LC Solvents[a]

solvent	$^1J_{CSi}$	$^1J_{CH}$	$^1J_{SiH}$	$^2J_{CH}$	$^2J_{SiH}$	$^3J_{HH(av)}$
ZLI 1167	−51.59(3)	122.514(12)	−194.449(11)	4.552(11)	7.962(12)	4.62(2)
ZLI 2806	−51.55(2)	122.42(2)	−194.670(5)	4.63(3)	7.989(12)	4.629(2)
ab initio	−60.50	115.74	−182.88	3.40	9.68	3.80[b]

[a] Values in Hz. The experimental values are measured at 350 K, where the liquid crystal is in the isotropic state, and the theoretical ab initio results are taken from the present RAS-II/HIII calculation. [b] (av) subscript means average coupling over two gauche- and one trans-position.

TABLE 3: Experimental D_{ij} Couplings (in Hz) of Methylsilane in Thermotropic Liquid Crystals ZLI 2806 and ZLI 1167

solvent T/K	ZLI 2806 315	ZLI 2806 305	ZLI 2806 298	ZLI 1167 310	ZLI 1167 300
$^1D_{CH}$	−98.10(4)	−117.89(3)	−127.13(5)	−115.18(3)	−124.22(2)
$^1D_{SiH}$	32.93(3)	39.68(2)	42.94(3)	37.93(3)	40.83(2)
$^1D_{CSi}$	−13.55(4)	−16.40(2)	−17.66(2)	−15.86(8)	−17.12(4)
$^2D_{HH}{}^a$	−157.588(11)	−189.487(7)	−204.51(2)	−184.141(8)	−197.809(7)
$^2D_{HH}{}^b$	−63.266(11)	−76.147(7)	−82.22(2)	−74.206(10)	−79.725(6)
$^2D_{CH}$	13.18(5)	15.85(3)	17.27(5)	15.43(3)	16.47(2)
$^2D_{SiH}$	−17.45(3)	−20.99(2)	−22.80(4)	−20.50(3)	−22.02(2)
$^3D_{HH}$	37.154(9)	44.631(6)	48.136(11)	43.435(7)	46.621(5)

[a] The $^2D_{HH}$ coupling within the CH_3 group. [b] The $^2D_{HH}$ coupling within the SiH_3 group.

TABLE 4: Fitted Coefficients of Eq 10 Determining the Geometry Parameters as Functions of Internal Rotation

P^a	a_0	$a_1{}^b$	$a_2{}^c$
$r_{CH}{}^d$	1.1149	0.0057	−0.0167
	1.0945	0.0105	−0.225
	1.0931	0.0315	−0.0100
r_{CSi}	1.8079	−0.123	−0.200
	1.8656	−0.215	−0.550
	1.8819	−0.494	−0.178
r_{SiH}	1.4630	−0.0073	−0.0167
	1.4932	0.0010	0
	1.4780	−0.0002	−0.0175
∠HCSi	111.771	−3.43	18.2
	111.676	−3.10	−1.08
	111.149	−10.2	−17.3
∠CSiH	110.922	−10.1	12.8
	110.753	−10.3	−8.89
	110.572	−16.1	−23.3

[a] The geometrical parameters in eq 10 corresponding to the equilibrium geometry are defined as $P_{theor} = a_0 + a_1 + a_2$. P_{iter}'s are given later in Table 6 (including also the fixed bond lengths, which are given in footnote *b* of the table). [b] Multiplied by 100. [c] Multiplied by 10 000. [d] The top values are for AM1, in the middle for PM3, and the lowest for ab initio/MP2 calculation.

internal (curvilinear) coordinate basis, where the interpolation was easy. In the internal coordinate basis, the force constants as a function of ϕ are given by

$$h(\phi) = h_0 + h_1 \cos(n\phi) + h_2 \cos(2n\phi) \qquad (11)$$

where $h(\phi)$ is a harmonic force constant. h_0, h_1, and h_2 were fitted to conform to the theoretical force constants at the calculated torsional angles. The period-dependent n has the value 1 for each parameter that corresponds to correlation between given CH and SiH vibrations. Otherwise $n = 3$ due to symmetry. In the case of FF taken from ref 11, we used our ab initio (MP2) results for relaxation of the geometry and for changes in FF (scaled with the adopted constants) during the internal rotation.

The anharmonic contributions were calculated with the AVIBR program[20] on the basis of diagonal cubic anharmonic stretching force constants that were estimated from the harmonic force field with $f_{rrr} = -3af_{rr}$, where $a = 2$ Å^{-1}.[40] This method is able to only partially correct for anharmonic effects and, thus, we do not give the experimental r_e geometry. We choose instead to make very small corrections in order to transform the corresponding $r_\alpha(T = 298, 305, 310,$ and 315 K) to the $r_\alpha(300$ K) geometry, where $T = 300$ K is the reference temperature in the present case. $r_\alpha(T)$ is defined by the thermal average positions of the atoms at the temperature T. At $T = 0$ K, the system is in the vibrational ground state and the average geometry, $r_\alpha(0$ K), is equal to the r_z geometry.[41] The latter is also an internally consistent geometry that is determinable especially with microwave and infrared spectroscopic methods. In LC NMR, r_α is the geometry corresponding to the dipolar couplings after corrections for harmonic vibrations and solvent-induced deformations. Usually it is very close to r_z, because at room temperature the occupancy of vibrational states other than the ground state is typically small.

In the present case, the changes, $\delta D^{ah} = D^{ah}(T) - D^{ah}(300$ K), in the anharmonic corrections to dipolar couplings are small (as seen in Table 5, where an example case of this and other corrections to the experimental anisotropic couplings is given), so that possible error in δD^{ah} as large as 20% is meaningless in the present case. In fact, this is the expected result, because at the small range of the present temperatures, the average geometries are close to each other.

The final optimization of the anisotropies (ΔA_{ij}) of the interaction tensors[10] acting on the CH, CSi, and SiH bonds, as well as that of the molecular geometry, was performed using the MASTER program as a Fortran-extension in the Matlab software.[42] The average $^3D_{HH}$ coupling was calculated as the mean of three $^3D_{HH}$ couplings at a given angle of internal rotation. The indirect contributions, except for CSi coupling, were very small as examplified in Table 5.

In the iteration procedure, we had to fix the r_{CSi} bond length for scaling the size of the system, as well as r_{CH}, because there was not enough information in the NMR data to obtain this parameter. The fixed values 1.864 and 1.095 Å, respectively, taken from ref 37 were obtained by "rigid rotor analysis" using rotational constants of the vibrational ground state, which means that the resulting geometry is of the r_0 type. Unfortunately, this geometry may differ slightly from r_α. Therefore, we give the relation between Δ^1J_{CSi} and r_{CH} in Table 6 (changes in r_{CSi} cause only new scaling of each parameter). The resulting r_α geometries are also given in the table and they are very close to each other when determined using different methods. However, the iterated geometrical parameters depend on the fixed values and, thus, their accuracy should not be overemphasized.

The results for the iterated geometry parameters and the anisotropy of $\mathbf{J}_{CSi}$ tensor are given in Table 6. The average Δ^1J_{CSi} changes by −10.7% between the semiempirical AM1 and PM3 methods. From PM3 to ab initio MP2 basis the change

TABLE 5: Example of Contributions to the Experimental Couplings[a]

coupling	D^a	D^h	δD^{ah}	D^d	$^1/_2J^{aniso}$	D^{calc}	D^{exp}	diff[b]	$^1/_2J^{aniso}/D^{\alpha c}$
$^3D_{HH}$	−85.909	−0.508	0.002	−0.395	0.018	−86.794	−86.869	−0.077	−0.02
$^2D_{HH(C)}$	389.415	−12.809	0.105	−8.316	−0.095	368.195	368.282	−0.019	−0.02
$^2D_{HH(Si)}$	148.303	−3.106	0.033	3.230	−0.033	148.395	148.411	−0.017	−0.02
$^2D_{CH}$	−30.780	0.237	−0.002	−0.351	0.005	−30.889	−30.860	0.030	−0.02
$^1D_{CH}$	256.964	−17.351	−0.023	−9.392	0.101	230.322	230.365	0.066	0.04
$^1D_{SiH}$	−74.194	3.584	0.005	−5.496	0.069	−76.036	−75.859	0.172	−0.09
$^2D_{SiH}$	41.554	−0.102	−0.001	−0.471	0.038	41.019	40.994	−0.025	0.09
$^1D_{CSi}$	32.847	0.114	−0.004	−0.030	−1.077	32.931	31.728	−0.123	−3.28

$S_{CSi}{}^d = 0.036087$; $\Delta A_{CH}{}^e = 1.91$; $\Delta A_{SiH}{}^e = -5.77$; $\Delta A_{CSi}{}^e = 3.86$

[a] Values in Hz for methylsilane, dissolved in liquid crystal ZLI 1167 at 310 K. D^α is the dipolar coupling in the r_α geometry at 300 K, D^h is due to harmonic vibrations, and δD^{ah} is the difference of the anharmonic contributions at 300 and 310 K. The indirect part ($^1/_2J^{aniso}$) is calculated on the basis of ab initio results except for the CSi coupling it is based on the current experimental results. [b] $D^{calc} - D^{exp}$. [c] The relative indirect contributions are given in percent. [d] The term defines the orientational parameter of the symmetry axis that is parallel with the CSi bond. [e] The anisotropies of the interaction tensors are given in 10^{-22} J.

TABLE 6: Molecular r_α Geometry at 300 K and the Anisotropy of Carbon−Silicon Spin−Spin Coupling in Methylsilane

LC	force field	r_{SiH}/Å	HCSi/deg	CSiH/deg	Δ^1J_{CSi}/Hz	$d\Delta^1J_{CSi}/dr_{CH}$[a]
ZLI 1167[b]	AM1[c]	1.514	110.69	111.20	−108	−22
	PM3[c]	1.514	110.71	111.21	−100	−22
	MP2[c]	1.520	110.81	111.30	−102	−15
	MP2[d]	1.516	110.85	111.21	−95	−12
	SCF[e]	1.514	110.83	111.15	−89	−9
ZLI 2806[b]	AM1[c]	1.511	110.81	110.99	−98	−12
	PM3[c]	1.508	110.86	110.94	−86	−13
	MP2[d]	1.514	110.95	111.02	−88	−9
	SCF[e]	1.515	110.92	111.03	−88	−12
average[f]					−89	−11
ab initio[g]					−59.32	

[a] The dependence of the fitted anisotropy on the fixed r_{CH} bond length is given in Hz/0.01 Å. [b] Basis for the indicated, iterated molecular geometry parameters: $r_{CH} = 1.095$ Å and $r_{CSi} = 1.864$ Å.[37] Δ^1J_{CSi} is constrained to be the same at different temperatures in a given LC. [c] The corrections due to anharmonic vibrations and the indirect contributions (except for CSi coupling) are ignored. [d] All contributions are taken into account. [e] The experimentally scaled harmonic force field in the equilibrium geometry is taken from ref 11, and other information from our MP2 calculations. [f] Mean of the results in the LC solvents, given by the force field denoted with *e*. [g] RAS−II/HIII calculation using r_0 geometry, given in ref 37.

is −2.0% and the "best" result using the scaled ab initio force field[11] (giving the best compatibility with the experimental harmonic frequencies) changes by further −2.8%. The significance of the other possible approximations (not included in the presented results) to Δ^1J_{CSi} are as follows: (1) classical calculation of the probability distribution as a function of the internal rotation angle (instead of a quantum mechanical one), +4.4%; (2) ignoring the relaxation of the geometry during internal rotation, −1.1%. These values imply that in the present case the internal rotation is described with the classical treatment to a reasonable accuracy and, contrary to ethane,[7] the relaxation of the geometry as a function of ϕ gives only small contribution to the D^{exp} couplings.

The theoretical result (discussed below), $\Delta^1J_{CSi} = -59.3$ Hz, is 33% smaller than the best experimental value, −89 Hz. The difference is slightly larger than in the experimentally very accurate isotropic values ($^1J_{CSi}{}^{exp} = -51.6$ Hz and $^1J_{CSi}{}^{theor} = -60.5$ Hz, see Table 2) where the difference is 17%. The reliable error limit estimation for the experimental value of Δ^1J_{CSi} is very complicated, but if we use an estimated error of 0.01 Å for the fixed $r_{\alpha,CH}$, we obtain the change of about 10 Hz in Δ^1J_{CSi}. This is most probably the dominant source of error.

Ab Initio Spin−Spin Coupling Tensors. The calculated spin−spin coupling constants and the tensor anisotropies are given in Table 7. The correlation convergence of the spin−spin coupling tensors can be investigated by comparing the RAS-I and RAS-II wave function levels. A substantial improvement in correlation treatment from RAS-I to RAS-II calculation produces typically relative changes up to 4% in the properties of **J** tensors. The coupling between two protons in silyl group, $^2J_{HH(Si)}$, is particularly sensitive to the correlation treatment as its sign changes. Although the relative changes also in Δ^2J_{CH} and $^3J_{HH(a)}$ are of the order of 10%, the absolute changes are maximally 4 Hz in all the mentioned parameters. These results indicate reasonably good correlation convergence of the parameters.

The basis set convergence of the spin−spin coupling tensors was examined at the RAS-II level. When using the HIII basis set instead of the more modest HII, the properties of **J** tensors change typically less than 10%. Although the tensor anisotropies and the $^2J_{HH(Si)}$ show larger relative changes than the other coupling constants, the order of magnitude of the absolute changes is 1 Hz in all cases except in the quite large $^1J_{CSi}$, which alters by 4 Hz. This is consistent with the previous application calculations and the recent systematic study[19] and supports the argument that HIII basis set provides reasonably good **J** tensors.

The FC mechanism gives the most significant contribution to the coupling constants, although in smaller constants this is due to the cancellation of DSO and PSO contributions. The SD contribution is generally very small, but in $^1J_{CSi}$ it is of the same order as DSO and PSO contributions. The typical dominance of SD/FC contribution in anisotropies is valid in the cases of Δ^1J_{CSi} and Δ^1J_{CH}. However, in other anisotropies also the DSO and PSO contributions are at least equally important, though they partially cancel each other in several cases. There is a slight difference in comparison with the case of ethane,[7] where the dominance of the SD/FC contribution was more obvious.

Compared with the experiment, the best (RAS-II/HIII) calculation underestimates $^2J_{CH}$ about 5.5%. The two-bond couplings $^2J_{CH}$ and $^2J_{SiH}$ are considerably smaller than one-bond couplings and therefore they actually differ less (1.7 Hz in maximum) than one-bond coupling from the experimental couplings. This is satisfactory, particularly as the two-bond couplings are known to be difficult to calculate reliably. In the average HH coupling between methyl and silyl groups, $^3J_{HH(av)}$, the underestimation is only about 1 Hz compared to experimental coupling. As expected, the most difficult object to calculate is, however, the $^1J_{CSi}$ tensor, because the 17.3% overestimation in coupling constant implies that a better description of either or both orbital and configuration spaces would be necessary. In the present system it seems that the improvement of both the basis set and the valence region

TABLE 7: Results of the MCSCF Calculations for the Spin−Spin Coupling Tensors in Methylsilane[a]

property[b]	RAS-I/HII[c]	RAS-II/HII[d]	RAS-II/HIII[e]	DSO	PSO	SD	FC	SD/FC
$^1J_{CSi}$	−66.95	−64.52	−60.50	−0.04	1.55	−1.35	−60.66	
Δ^1J_{CSi}	−59.97	−60.23	−59.32	−3.17	−0.99	−2.14		−53.02
$^1J_{CH}$	118.40	116.89	115.74	0.56	1.53	−0.10	113.75	
Δ^1J_{CH}	8.37	8.12	7.10	−6.52	4.08	0.22		9.31
$^1J_{SiH}$	−186.50	−182.88	−182.88	−0.12	0.58	0.12	−183.45	
Δ^1J_{SiH}	5.77	5.75	5.81	6.41	−2.55	−0.14		2.09
$^2J_{CH}$	3.36	3.36	3.40	−0.31	0.24	0.01	3.47	
Δ^2J_{CH}	0.40	0.44	0.41	1.31	−0.66	0.01		−0.25
$^2J_{SiH}$	11.01	10.76	9.68	0.21	0.03	−0.16	9.60	
Δ^2J_{SiH}	3.14	3.14	2.56	−3.53	1.33	−0.15		4.91
$^2J_{HH(C)}$	−17.29	−16.57	−15.24	−2.68	2.94	0.37	−15.87	
$\Delta^2J_{HH(C)}$	−7.92	−7.83	−7.33	−7.77	5.18	−0.41		−4.33
$^2J_{HH(Si)}$	−0.29	1.52	2.52	−2.11	1.77	0.06	2.80	
$\Delta^2J_{HH(Si)}$	−2.77	−2.70	−1.96	−4.41	3.20	−0.01		−0.73
$^3J_{HH(a)}$	0.69	0.62	0.66	−0.66	0.56	0.03	0.74	
$\Delta^3J_{HH(a)}$	1.45	1.44	1.04	2.98	−2.19	0.02		0.23
$^3J_{HH(b)}$	9.41	9.43	10.06	−2.53	2.32	0.00	10.27	
$\Delta^3J_{HH(b)}$	1.57	1.56	1.61	0.74	−0.43	−0.04		1.34
$^3J_{HH(av)}$	3.60	3.56	3.80					
$\Delta^3J_{HH(av)}$	1.49	1.48	1.23					

[a] Results in Hz. Calculations performed at the r_0 geometry: $r_{CH} = 1.095$ Å, $r_{CSi} = 1.864$ Å, ∠HCSi = 110.88°, and ∠CSiH = 110.41°.[37] The anisotropy is defined as $\Delta J = J_{zz} - {}^1/_2(J_{xx} + J_{yy})$ with the CSi bond at the *z* direction. The contributions of the different physical mechanisms to the calculated tensors are indicated for the RAS−II/HIII calculation. [b] (a) and (b) subscripts denote coupling between hydrogens belonging to methyl and silyl groups at gauche- and trans-position to each other, respectively. (av) subscript means average coupling over two gauche- and one trans-position. [c] Total energy −330.483 116 Ha. [d] Total energy −330.557 097 Ha. [e] Total energy −330.593 950 Ha.

correlation description has an effect in the same direction and therefore there is no possibility to utilize error cancellation. The apparent relative similarity of the results from our two active spaces (differing in the treatment of electron correlation in the valence region) and two basis sets seems to point to an earlier suggestion[43] that the neglect of core correlation (in the Si atom in the present system) may be largely responsible for the error. In addition, comparison of ab initio and LC NMR results is fully justified only when the former are performed at the r_α geometry, and not at the r_0 geometry as done presently (nor at the r_e geometry as often done). As previously noted, also the experimental determination of Δ^1J_{CSi} involves many approximations. However, it is justified to state that the calculated results are at least satisfactory for all couplings.

To our knowledge, there are only few first principles calculations of **J** tensors for methylsilane. The first article was published by Fronzoni and Galasso,[44] who used the EOM method and obtained the values $^1J_{SiH} = -193.63$ Hz and $^1J_{CSi} = -54.63$ Hz, which are close to the experimental values. The small 6-31G** basis set used in the calculations allows speculation about possible error cancellation. Malkina et al.[43] applied their DFT method[45] to the determination of different silicon spin−spin coupling constants and they give the result $^1J_{SiH} = -196.94$ Hz for methylsilane, which is in excellent agreement with the experiment. Whereas the DFT method has severe problems for couplings involving centers with lone pairs,[43,45] it has been shown to perform extremely well for couplings between the nuclei of group 14 atoms and/or hydrogen, as in the present case. Neither of the two earlier papers reported the tensorial properties of the couplings, which form our main topic in the present contribution.

The principal values of the principal axis system (PAS) for all the theoretical **J** tensors in methylsilane are listed in Table 8. The orientations of the principal axis are described in the footnote. The principal axes are plotted at one of the coupled nuclei in Figure 1.

When comparing the **J** tensor properties between molecules having different symmetry, one is generally forced to use the PAS of the tensors. Moreover, if the object of interest is purely

TABLE 8: Theoretical Principal Values and the Orientation of the Principal Axis System of the J Tensors in Methyl Silane (CH_3SiH_3)[a]

coupling[b]	J_{33}	J_{22}	J_{11}	ΔJ_{ij}[c]
$^1\mathbf{J}_{CSi}$[d]	−100.05	−40.73	−40.73	−59.32
$^1\mathbf{J}_{CH}$[e]	125.63	124.85	96.73	14.84
$^1\mathbf{J}_{SiH}$[f]	−195.16	−176.97	−176.50	−18.42
$^2\mathbf{J}_{CH}$[g]	3.84	3.58	2.79	0.65
$^2\mathbf{J}_{SiH}$[h]	12.06	11.41	5.56	3.58
$^2\mathbf{J}_{HH(C)}$[i]	−26.49	−9.73	−9.50	−16.88
$^2\mathbf{J}_{HH(Si)}$[j]	3.72	3.69	0.15	1.80
$^3\mathbf{J}_{HH(a)}$[k]	1.45	0.60	−0.06	1.19
$^3\mathbf{J}_{HH(b)}$[l]	11.26	9.80	9.13	1.80

[a] Principal values in Hz. The principal values have been ordered according to $|J_{11}| \le |J_{22}| \le |J_{33}|$. The principal axis systems are shown in Figure 1. [b] (a) and (b) subscripts denote coupling between hydrogens belonging to methyl and silyl groups at gauche- and trans-position to each other, respectively. [c] Anisotropy is defined as $\Delta J_{ij} = J_{33} - {}^1/_2(J_{11} + J_{22})$. [d] J_{33} is directed along the CSi bond. [e] J_{11} and J_{22} are in the HCSi plane and J_{11} makes an angle of 2.4° with the CH bond toward the Si atom [f] J_{33} makes an angle of 0.9° with the SiH bond toward the C atom in the CSiH plane. J_{22} is also in this plane. [g] Coupling is to the proton where the PAS of the $^2J_{HH(Si)}$ tensor is shown. J_{33} makes an angle of 22.6° with the CH direction away from silane atom in the CSiH plane. J_{22} is in the same plane. [h] J_{22} makes an angle of 20.8° with SiH direction away from Si atom in the HCSi plane. Also J_{11} is in this plane. [i] J_{11} is directed along the HH direction in the HCH plane and J_{33} is practically perpendicular with this plane. [j] J_{33} is directed along the HH direction in the HSiH plane and J_{22} makes an angle of 3.4° with this plane toward the methyl group. [k] Coupling is to the proton where the PAS of the $^2\mathbf{J}_{SiH}$ is located. J_{33} makes an angle of 9.6° with the HH direction and an angle of 10.0° with the HSiC plane. For J_{11}, the same angles are 80.4° and 39.1°, respectively. [l] Coupling is to the proton where the PAS of the $^2\mathbf{J}_{SiH}$ tensor is shown. J_{33} is of 24.2° from the HH direction toward the carbon atom in the HSiCH plane. Also J_{22} is in this plane.

the electronic coupling regardless of the gyromagnetic ratios of the coupled nuclei, the comparison has to be carried out using reduced spin−spin couplings, $\mathbf{K}_{ij}$, which are related to the $\mathbf{J}_{ij}$ through

$$\mathbf{J}_{ij} = (1/2\pi)\hbar\gamma_i\gamma_j\mathbf{K}_{ij} \qquad (12)$$

TABLE 9: Reduced Spin−Spin Coupling Constants and Anisotropies in the Principal Axis System[a]

	K_{ij}		ΔK_{ij}[c]	
property[b]	C_2H_6	CH_3SiH_3	C_2H_6	CH_3SiH_3
$^1\mathbf{K}_{CSi}$		100.73		98.75
$^1\mathbf{K}_{CC}$	51.10		42.25	
$^1\mathbf{K}_{CH}$	39.66	38.31	4.31	4.91
$^1\mathbf{K}_{SiH}$		76.57		7.71
$^2\mathbf{K}_{CH}$	−1.76	1.13	−0.81	0.22
$^2\mathbf{K}_{SiH}$		−4.05		−1.50
$^2\mathbf{K}_{HH(C)}$	−1.18	−1.27	−1.42	−1.40
$^2\mathbf{K}_{HH(Si)}$		0.21		0.15
$^3\mathbf{K}_{HH(a)}$	0.29	0.06	0.14	0.10
$^3\mathbf{K}_{HH(b)}$	1.22	0.84	0.27	0.15

[a] Properties in 10^{19} T^2 J^{-1}. The reduced spin−spin coupling constants and anisotropies of the methylsilane and ethane are derived from the present RAS−II/HIII calculation and the best theoretical data in ref 7, respectively. [b] See footnote *b* in Table 8. [c] Anisotropy is defined as $\Delta K_{ij} = K_{33} - {}^1/_2(K_{11} + K_{22})$, where the principal values have been ordered as $|K_{33}| \geq |K_{22}| \geq |K_{11}|$.

TABLE 10: Relative Harmonic Contributions D^h/D^{eq} Given by Different Force Fields[a]

coupling	AM1	PM3	MP2	ref 11[b]
$^3D_{HH}$	−0.26	−0.34	−0.59	−0.56
$^2D_{HH(C)}$	−2.68	−2.95	−3.61	−3.38
$^2D_{HH(Si)}$	−2.49	−2.04	−2.29	−2.07
$^2D_{CH}$	−1.12	−0.78	−0.78	−0.77
$^1D_{CH}$	−5.41	−5.86	−6.85	−6.92
$^1D_{SiH}$	−6.34	−5.06	−4.90	−4.45
$^2D_{SiH}$	−0.28	−0.19	−0.25	−0.27
$^1D_{CSi}$	0.41	0.40	0.33	0.35

[a] In percent at the equilibrium value $\phi = 0$ of internal rotation. [b] Scaled ab initio force constants.

The comparison of the $\mathbf{K}_{ij}$ tensors between methylsilane and ethane[7] is interesting as the electronic structure is expected to be quite similar at least from the symmetry point of view. Table 9 shows the coupling constants and anisotropies of the $\mathbf{K}_{ij}$ tensors in the PAS. The $^1\mathbf{K}_{CSi}$, $^1\mathbf{K}_{SiH}$, and $^2\mathbf{K}_{SiH}$ couplings in methylsilane are twice as large as the $^1\mathbf{K}_{CC}$, $^1\mathbf{K}_{CH}$, and $^2\mathbf{K}_{CH}$ couplings in ethane, respectively. As expected, the coupling constants as well as the anisotropies of the $^1\mathbf{K}_{CH}$ and $^2\mathbf{K}_{HH(C)}$ tensors are very similar between the molecules. It is also noticeable that in the couplings over two bonds the sign changes when the atom in the coupling path is silicon instead of carbon as one can see in both the $^2\mathbf{K}_{CH}$ and the $^2\mathbf{K}_{HH}$ couplings.

Discussion

Comparing the different methods, there are no significant differences between the geometries given by using different harmonic force fields (see Table 6). Possibly the most clear distinction is seen in the directly comparable relative harmonic contributions, D^h/D^{eq}, given in Table 10.

For most couplings, the corrections given by our ab initio MP2 calculation without scaling and most probably the best of the current force fields, i.e., that given in ref 11 (scaled SCF method), are in good mutual agreement, whereas the semiempirical AM1 and PM3 results deviate from these. However, also semiempirical force fields correct for most of the harmonic vibrational effects and, consequently, it is much better to use them than to ignore the vibrational contributions altogether. It must be noted that with each set of analysis parameters, we used the same probability distribution as a function of internal rotation; i.e., the rotational barrier was not adopted from the calculations. The theoretical barriers would have been 121 cm^{-1} in AM1, 201 cm^{-1} in PM3, and 528 cm^{-1} in MP2, whereas the experimental value used is 603 cm^{-1}.[23] At least in the present case, this implies that semiempirical methods may not be reliable in the case of properties concerning large-amplitude motions or for structural energetics far from the equilibrium geometry.

For the system at hand, the indirect contribution is very significant as it gives the dominant correction to the experimental CSi coupling (see Table 5). If the experimental $^1D_{CSi}$ is used in the study of orientational order parameter, S_{CSi}, omitting the correction due to indirect coupling contribution would lead to an error of −3.3% (the ab initio result leads to −2.2%). When determining the r_{CSi} bond length, the corresponding error would be +1.1%. Probably the situation remains in other molecules that include CSi single bonds. The principal axis directions are generally difficult to guess, but the **J** tensors in a molecule-fixed frame appear to be directly transferable to other molecules owing to the same local symmetry for the tensor. This is indicated for example by a comparison of the ab initio $^1J_{CH}$ tensors of C_2H_6,[7] CH_3F,[5] and CH_3SiH_3. The Δ^1J_{CH} values in the respective order are 6.0, 6.1, and 8.1 Hz (symmetry axis used as the *z* axis in each molecule). The values for $\Delta^2J_{HH(C)}$ are −8.3, −10.5, and −7.3 Hz in the same molecule-fixed coordinate system. Especially, $^1\mathbf{J}_{CH}$ is very close to being cylindrically symmetric in the bond direction and, therefore, the relative indirect contribution, ${}^1/_2{}^1J_{CH}{}^{aniso}/{}^1D_{CH}{}^{eq}$, is nearly orientation-independent. The ratio is nearly the same in different molecules and, therefore, it may be used as an approximate a priori correction for other molecules, for which $^1\mathbf{J}_{CH}$ is otherwise unknown. Correspondingly, in the case of the $^1\mathbf{J}_{CF}$ tensor,[4,5] the indirect contribution to $^1D_{CF}{}^{exp}$ coupling is partially removable by multiplying the $^1D_{CF}{}^{eq}$ with 1.01 (${}^1/_2{}^1J_{CF}{}^{aniso} \approx -{}^1D_{CF}{}^{eq}/100$, compare with eq 3) in the analysis of the molecular geometry and orientation. Δ^1J_{CC} appears between 26.5 and 47.5 Hz in the CC internuclear direction (in the case of planar molecules also $^1J_{CC,xx} - {}^1J_{CC,yy}$ possesses a nonzero value, which is systematically about −40 Hz, with *z* axis in the CC direction and *x* axis in the molecular plane).[4,6,7] Especially, the theoretical result for Δ^1J_{CC} is 32.1 Hz in ethane[7] and 36.6 Hz in acetonitrile,[12] both possessing CC single bond. Therefore, most probably also $\Delta^1J_{CSi}{}^{aniso}$ remains fairly constant in different molecules with CSi single bond and it may be used as an a priori correction to $^1D_{CSi}{}^{exp}$.

Conclusions

The spin−spin coupling tensor, $^1\mathbf{J}_{CSi}$, for methylsilane is determined experimentally by utilizing liquid crystal NMR method and, along with also all the other **J** coupling tensors of the molecule, theoretically with ab initio MCSCF linear response calculations. The best theoretical and experimental results are in fair mutual agreement. The respective anisotropies of the tensor are −89 ± 10 Hz and −59.3 Hz, whereas the values for the $^1J_{CSi}$ coupling constant are −51.6 and −60.5 Hz, respectively. The anisotropic part of the indirect coupling, ${}^1/_2{}^1J_{CSi}{}^{aniso}$, is found to contribute to the corresponding experimental anisotropic coupling $^1D_{CSi}{}^{exp}$ coupling significantly, by about 3%. In the analysis of the experimental data, the sensitivity of the contributions due to harmonic vibrations to the method of calculating the harmonic force field was tested by applying semiempirical and ab initio methods. The nonscaled ab initio MP2 calculation is found to give sufficient accuracy for the harmonic force field, used in LC NMR, but also the semiempirical FF corrects for most of the vibrational effects. However, in the latter case the parameters associated with the large-amplitude torsional motion are poorly determined. The present

results, together with earlier experience, suggest that the ab initio MCSCF calculations are able to produce qualitatively correct indirect contributions to the experimental dipolar couplings at least for small probe molecules containing silicon. Explicit treatment of core correlation in second-row atoms may be necessary for quantitatively correct spin−spin couplings to these nuclei when the MCSCF method is used. The **J** tensors are found to be transferable from one molecule to another containing the similar structural unit, and the necessary harmonic force field can be determined with reasonable accuracy with fast semiempirical calculations, although the ab initio method is preferred. The transferability of the **J** tensors may be exploited in order to produce approximate corrections to the corresponding D^{exp} couplings, which thus become useful for the determination of molecular orientation and geometry.

Acknowledgment. The authors are grateful to the Academy of Finland for financial support. J.K. expresses his gratitude to the Finnish Cultural Foundation and Oulu University Foundation for grants. P.L. acknowledges grants from the Finnish Cultural Foundation and the Pohjois-Pohjanmaa Fund of the Finnish Cultural Foundation. The computational resources were supplied by Center for Scientific Computing, Espoo, Finland.

References and Notes

(1) Lounila J.; Jokisaari, J. *Prog. NMR Spectrosc.* **1982**, *15*, 249.

(2) Jokisaari, J. *Encyclopedia of NMR Spectroscopy*; Grant, D., Harris, R. K., Eds.; John Wiley & Sons: New York, 1996; Vol. 2, p 839.

(3) Wasylishen, R. E. *Encyclopedia of NMR Spectroscopy*; Grant, D., Harris, R. K., Eds.; John Wiley & Sons: New York, 1996; Vol. 3, p 1685.

(4) Vaara, J.; Kaski, J.; Jokisaari, J. *J. Phys. Chem. A* **1999**, *103*, 5675.

(5) Lantto, P.; Kaski, J.; Vaara, J.; Jokisaari, J. *Chem. Eur. J.*, in press.

(6) Kaski, J.; Vaara, J.; Jokisaari, J. *J. Am. Chem. Soc.* **1996**, *118*, 8879.

(7) Kaski, J.; Lantto, P.; Vaara, J.; Jokisaari, J. *J. Am. Chem. Soc.* **1998**, *120*, 3993.

(8) Prestegard, J. H. *Nature Struct. Biol.* **1998**, *5*, 517, and references therein.

(9) Sýkora, S.; Bösiger, H.; Diehl, P. *J. Magn. Reson.* **1979**, *36*, 53.

(10) (a) Lounila, J.; Diehl, P. *J. Magn. Reson.* **1984**, *56*, 254. (b) *Mol. Phys.* **1984**, *52*, 827. (c) Lounila, J. *Mol. Phys.* **1986**, *58*, 897.

(11) Duncan J. L.; Ferguson, A. M. *Spectrochim. Acta* **1996**, *52A*, 1515.

(12) Barszczewicz, A.; Helgaker, T.; Jaszuński, M.; Jørgensen, P.; Ruud, K. *J. Magn. Reson. A* **1995**, *114*, 212.

(13) Vaara, J.; Kaski, J.; Jokisaari, J.; Diehl, P. *J. Phys. Chem. A* **1997**, *101*, 5069, 9185.

(14) Pyykkö, P. *Chem. Phys.* **1977**, *22*, 289. Pyykkö, P.; Wiesenfeld, L. *Mol. Phys.* **1981**, *43*, 557.

(15) Aucar G. A.; Oddershede, J. *Int. J. Quantum Chem.* **1993**, *47*, 425.

(16) Kirpekar, S.; Jensen, H. J. Aa.; Oddershede, J. *Theor. Chem. Acta* **1997**, *95*, 35. Vaara, J.; Ruud, K.; Vahtras, O. *J. Comput. Chem.* **1999**, *20*, 1314.

(17) Grossmann, G.; Potrzebowski, M. J.; Fleischer, U.; Krüger, K.; Malkina, O. L.; Ciesielski, W. *Solid State NMR* **1998**, *13*, 71.

(18) Olsen J.; Jørgensen, P. *J. Chem. Phys.* **1985**, *82*, 3235. Jørgensen, P.; Jensen, H. J. Aa.; Olsen, J. *J. Chem. Phys.* **1988**, *89*, 3654. Olsen, J.; Yeager, D. L.; Jørgensen, P. *J. Chem. Phys.* **1989**, *91*, 381.

(19) Helgaker, T.; Jaszuński, M.: Ruud, K.; Górska, A. *Theor. Chem. Acc.* **1998**, *99*, 175.

(20) Lounila, J.; Wasser, R.; Diehl, P. *Mol. Phys.* **1987**, *62*, 19.

(21) Wasser, R.; Kellerhals, M.; Diehl, P. *Magn. Reson. Chem.* **1989**, *27*, 335.

(22) Duncan, J. L.; Ferguson, A. M.; McKean, D. C. *J. Mol. Spectrosc.* **1994**, *168*, 522.

(23) Schroderus, J.; Ozier, I.; Moazzen-Ahmadi, N., manuscript in preparation.

(24) Ball, D. F.; Goggin, P. L.; McKean, D. C.; Woodward, L. A. *Spectrochim. Acta* **1960**, *16*, 1358.

(25) Laatikainen, R.; Niemitz, M.; Weber, U.; Sundelin, J.; Hassinen, T.; Vepsäläinen, J. *J. Magn. Reson. A* **1996**, *120*, 1.

(26) Frich, M. J.; Trucks, G. W.; Schlegel, H. B.; Gill, P. M. W.; Johnson, B. G.; Robb, M. A.; Cheeseman, J. R.; Keith, T.; Petersson, G. A.; Montgomery, J. A.; Raghavachari, K.; Al-Laham, M. A.; Zakrzewski, V. G.; Ortiz, J. V.; Foresman, J. B.; Cioslowski, J.; Stefanov, B. B.; Nanayakkara, A.; Challacombe, M.; Peng, C. Y.; Ayala, P. Y.; Chen, W.; Wong, M. W.; Andres, J. L.; Replogle, E. S.; Gomberts, R.; Martin, R. L.; Fox, D. J.; Binkley, J. S.; Defrees, D. J.; Baker, J.; Stewart, J. P.; Head-Gordon, M.; Conzalez, C.; Pople, J. A. *Gaussian 94*, *Revision E.2*; Gaussian, Inc.: Pittsburgh, PA, 1995.

(27) Dewar, M. J. S.; Zoebisch, E. G.; Healy, E. F.; Stewart, J. J. P. *J. Am. Chem. Soc.* **1985**, *107*, 3902; *J. Mol. Struct.* **1988**, *180*, 1; **1989**, *187*, 1.

(28) Stewart, J. J. P. *J. Comput. Chem.* **1989**, *10*, 209; **1991**, *12*, 320.

(29) Møller, Chr.; Plesset, M. S. *Phys. Rev.* **1934**, *46*, 618.

(30) Vahtras, O.; Ågren, H.; Jørgensen, P.; Jensen, H. J. Aa.; Padkjær, S. B.; Helgaker, T. *J. Chem. Phys.* **1992**, *96*, 6120.

(31) Helgaker, T.; Jensen, H. J. Aa.; Jørgensen, P.; Olsen, J.; Ruud, K.; Ågren, H.; Andersen, T.; Bak, K. L.; Bakken, V.; Christiansen, O.; Dahle, P.; Dalskov, E. K.; Enevoldsen, T.; Fernandez, B.; Heiberg, H.; Hettema, H.; Jonsson, D.; Kirpekar, S.; Kobayashi, R.; Koch, H.; Mikkelsen, K. V., Norman, P.; Packer, M. J.; Saue, T.; Taylor, P. R.; Vahtras, O. *Dalton, an Ab Initio Electronic Structure program*, *Release 1.0*, 1997. See http://www.kjemi.uio.no/software/dalton/dalton.html.

(32) Helgaker, T.; Jaszuński, M.; Ruud, K. *Chem. Rev.* **1999**, *99*, 293.

(33) Åstrand, P.-O.; Mikkelsen, K. V.; Jørgensen, P.; Ruud, K.; Helgaker, T. *J. Chem. Phys.* **1998**, *108*, 2528.

(34) Huzinaga, S. *Approximate Atomic Functions*; University of Alberta: Edmonton, Canada, 1971.

(35) Kutzelnigg, W.; Fleischer, U.; Schindler, M. *NMR Basic Principles and Progress*; Diehl, P., Fluck, E., Günther, H., Kosfeld, R., Seelig, J., Eds.; Springer-Verlag: Berlin, 1990; Vol. 23.

(36) Guilleme J.; San Fabián, J. *J. Chem. Phys.* **1998**, *109*, 8168.

(37) Wong, M.; Ozier, I. *J. Mol. Spectrosc.* **1983**, *102*, 89.

(38) Marsmann, H. C. *Encyclopedia of NMR Spectroscopy*; Grant, D., Harris, R. K., Eds.; John Wiley & Sons: New York, 1996; Vol. 7, p 4386.

(39) Marsmann, H. *NMR Basic Principles and Progress*; Diehl, P., Fluck, E., Kosfeld, R., Eds.; Springer-Verlag: Berlin, 1981; Vol. 17.

(40) Kuchitsu, K.; Morino, Y. *Bull. Chem. Soc. Jpn.* **1965**, *38*, 805.

(41) Gordy W.; Cook, R. L. *Microwave Molecular Spectra*, *Techniques of Chemistry*, 3rd ed.; John Wiley & Sons: New York, 1984; Vol. XVIII.

(42) Matlab version 5.3.0.10183. See http://www.mathworks.com.

(43) Malkina, O. L.; Salahub, D. R.; Malkin, V. G. *J. Chem. Phys.* **1996**, *105*, 8793.

(44) Fronzoni, G.; Galasso, V. *Chem. Phys.* **1986**, *103*, 29.

(45) Malkin, V. G.; Malkina, O. L.; Salahub, D. R. *Chem. Phys. Lett.* **1994**, *221*, 91.